High-resolution magneto-optic measurements with a Sagnac interferometer (invited)

A. Kapitulnik, J. S. Dodge, and M. M. Fejer
Department of Applied Physics, Stanford University, Stanford, California 94305

A technique for measuring the Faraday effect and the magneto-optic Kerr effect has been developed. In a Sagnac interferometer, two optical beams follow identical paths in opposite directions. Effects which break time-reversal symmetry, such as magneto-optic effects, will cause destructive interference between the two beams. By measuring the phase shift between circular polarization states reflected from a magnetized sample, the polar magneto-optic Kerr effect is measured to an accuracy of 3 μrad, with a spatial resolution of 2 μm. The interferometric technique provides a number of advantages over conventional polarizer methods, including insensitivity to linear birefringence, the ability to completely determine the magnetization vector in a region, and the ability to sensitively measure magneto-optic effects without an external field. It is also shown that this device has great potential if incorporated into a near-field optical device. Some of the considerations for the design of a near-field Sagnac magneto-optic sensor are introduced and the advantages of the device are discussed. Some preliminary experiments are shown.

I. INTRODUCTION

Magneto-optic studies of magnetic films and of surface magnetism in bulk materials is very common.[1] In particular the surface magneto-optic Kerr effect (SMOKE)[2] has recently been refined to a state where selected systems can be studied to a submonolayer level. The Kerr effect, like all other magneto-optic effects,[3] originates from spin-orbit coupling. Its net effect is to produce a rotation of the polarization axes as well as a slight ellipticity in linearly polarized light reflected from a magnetized surface. The amount of Kerr rotation is directly proportional to the magnetization in the film, and thus provides an excellent method to study magnetism. In bulk materials, Kerr rotation and ellipticities can be as high as 10^{-2} rad (for a measurement of a metal using visible light with an optical penetration depth of $\sim$100 Å, this implies a specific rotation of $\sim 10^4$ rad/cm). For very thin films, the effect can be reduced substantially, hence restricting the materials and configurations that can be studied.

Magneto-optics is also discussed in the context of high-density data storage, where bits are represented as domains in a magnetic film which has strong perpendicular anisotropy. Data are written optically by locally heating the film above its Curie temperature with a laser, and aligning a domain with an applied magnetic field. The data are then read by means of the polar Kerr effect. A diffraction-limited optical device is capable of handling cell sizes as low as $(1\ \mu\text{m})^2$. In this limit, detailed imaging of the domain structure is beyond the capabilities of conventional polarized light microscopy, and currently we must turn to electron microscopes for high-resolution images. Near-field optical microscopy, operating in reflection with magneto-optic contrast, may be particularly useful in guiding the engineering of such storage materials. We might further imagine a near-field magneto-optic read-write system, which could push the minimum cell size down to the order of $\sim$(500 Å),[2] hence increasing the storage density to more than 10^{10} bits/in.[2]; however, to date there are no magneto-optic devices which are working both in reflection and in the near-field region.

Recently we have demonstrated[4–7] the use of a Sagnac interferometer for the measurement of Faraday and Kerr effects. Three instruments were built to operate at 1060, 672, and 840 nm. One important advantage of these instruments over conventional SMOKE is that they are sensitive only to broken time-reversal symmetry effects while completely rejecting linear birefringence and optical activity. Our first instrument was built using an existing fiber-optic gyroscope (λ=1060 nm). For measurements of the Faraday rotation angle, the sensitivity achieved was 3 $\mu\text{rad}/\sqrt{\text{Hz}}$. We have since built instruments (λ=672 and 840 nm), designed more specifically for magneto-optic studies, which are slightly modified from the original with a shorter Sagnac loop. These instruments work in both transmission and reflection to measure both the Faraday and Kerr effects. The sensitivity achieved has been 2 $\mu\text{rad}/\sqrt{\text{Hz}}$. The Sagnac magneto-optic sensor (SMOS) was first developed in the search for anyon superconductivity in high-temperature superconductors;[4] we are currently giving more attention to its use for characterization of magnetic materials. An important measurement was the observation of free radicals in biological molecules.[7] In this experiment we showed the versatility of SMOS. The sensitivity found was comparable to electron-spin resonance (ESR), the only other technique used to look for free radicals; however, the sensitivity is not the only advantage of SMOS. As we explain below, SMOS is able to measure absolute magnetization, hence avoiding the need for external field modulation. Moreover, we show that SMOS is capable

 0021-8979/94/75(10)/6872/6/$6.00

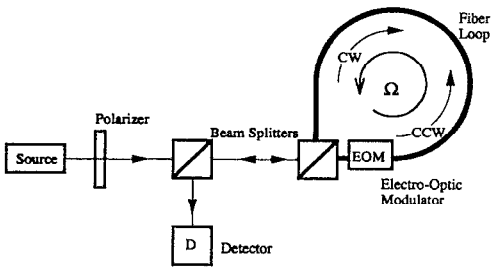

FIG. 1. Basic configuration of a Sagnac interferometer. Ω is the angular frequency of rotation of the loop.

of fully determining the state of magnetization in a sample region, and should provide a unique way to probe surface anisotropies.

II. SAGNAC INTERFEROMETER

Figure 1 shows a schematic of a basic Sagnac interferometer. The beam of light from the source enters a beam splitter, which sends half of the light clockwise (CW) and the other half counterclockwise (CCW) around a fiber loop. The two beams will come to the beam splitter after one turn and combine to constructively interfere at the detector. This is the Sagnac loop at rest and if we assume that the fiber allows one and only one path through the loop, it is completely reciprocal. If the loop is now rotated at a constant angular velocity Ω, reciprocity is no longer preserved. The rotation creates a difference in path length between the two counterpropagating beams, so that there will be a slight phase shift, the so-called Sagnac effect, introduced between them. This phase shift is translated into an intensity change when the two beams interfere at the detector. The phase shift will be proportional to the area enclosed by the loop, so with a fiber-optic loop the sensitivity to mechanical rotation can be increased by adding more windings.[8]

As described above, small changes in path length will lead to intensity changes proportional to the phase difference squared, which will in turn lead to poor sensitivity to small phase shifts. Typically the interferometer will be biased onto the linear portion of the interference curve to increase the sensitivity. In principle, this can be done by introducing a nonreciprocal element into the loop which creates a stable $\pi/4$ phase shift between the two beams. However, in practice, a dynamic biasing system is easier to engineer. In Fig. 1 we show one common bias technique, in which an electro-optic phase modulator is placed at one end of the loop. Although the phase modulator is a reciprocal device, we take advantage of the finite time it takes light to travel around the loop to create a nonreciprocal phase shift between beams which pass through the modulator at different times. With a sinusoidal phase modulation, the first-harmonic component of the detected intensity may be measured with a lock-in amplifier. For a small nonreciprocal phase shift $\Delta\phi_s$ and an average detected intensity I_0, the first harmonic is proportional to $k_1 I_0 \sin(\Delta\phi_s)$, where k_1 is a constant which depends on the phase modulation amplitude. Maximum sensitivity is achieved for a modulation frequency of $f=c/2L$, where L is the path length of the loop. Additionally, parasitic effects due to imperfections in the phase modulator will be significantly reduced near this frequency. Consequently, although the SMOS is not designed for mechanical rotation measurements, we must maintain a finite loop length of about 30 m in order to keep the modulation frequency in the MHz range.

To achieve sensitivity to magnetic substances, one would like to measure the asymmetry between the CW and the CCW beams induced by the nonreciprocity (broken time-reversal symmetry) resulting from magnetism. To do this, we "break" a (completely reciprocal) Sagnac loop, then introduce bulk optics into the optical path to allow us to probe a sample. More specifically, we use wave plates to create two polarization states which will lead to the maximum nonreciprocal phase shift upon interaction with a magnetized sample. The simplest geometries for describing the operation of the SMOS are those in which the sample exhibits no linear birefringence, and the direction of beam propagation is both collinear with the magnetization and normal to the sample surface. This corresponds to the polar Kerr effect in reflection and the Faraday effect in transmission. Choosing the z axis as the direction of beam propagation, the conductivity tensor for the material may be written in the form

$$\sigma(\mathbf{M}\|\hat{\mathbf{z}})=\begin{pmatrix}\sigma_{xx} & \sigma_{xy} & 0\\ -\sigma_{xy} & \sigma_{xx} & 0\\ 0 & 0 & \sigma_{xx}\end{pmatrix}. \tag{1}$$

For both of these geometries, circular polarization states are the appropriate basis for describing magneto-optic effects.[9] Transforming the electric-field vector to a circular basis diagonalizes the conductivity tensor and gives slightly different diagonal elements $\sigma_{\pm}=\sigma_{xx}\pm i\sigma_{xy}$ for the two basis states. The reflectance and the transmittance of the material is affected similarly, so that we may measure a difference in both the relative phase shift and the absorption between the two states. It is important to note here that this phase shift is nonreciprocal, unlike the phase shifts induced by linear birefringence or optical activity, since the magnetization breaks time reversal symmetry. It is precisely this nonreciprocity which allows us to measure magneto-optic effects using SMOS.

The most common way to measure these effects is to direct linearly polarized light at the sample and measure the polarization state of the returning light, so the literature commonly refers to the phase shift as "rotation," denoted by θ, and the differential absorption as "ellipticity," denoted by ϵ. We refer to the nonreciprocal phase shift (NRPS) throughout this article, and denote it by $\Delta\phi$. In the perpendicular geometries described above, $\Delta\phi=2\theta$, but in general the phase shift is a function of both the rotation and the ellipticity. To measure the NRPS, we compare two states with opposing angular momentum vectors, so that one is parallel to the magnetization and the other antiparallel. In transmission, this corresponds to states of the same handedness, and in reflection the appropriate states have opposite handednesses, where handedness is defined with respect to the direction of propagation [Fig. 2(a)]. When configured in this way, the SMOS is sensitive only to Faraday or Kerr rotation, not el-

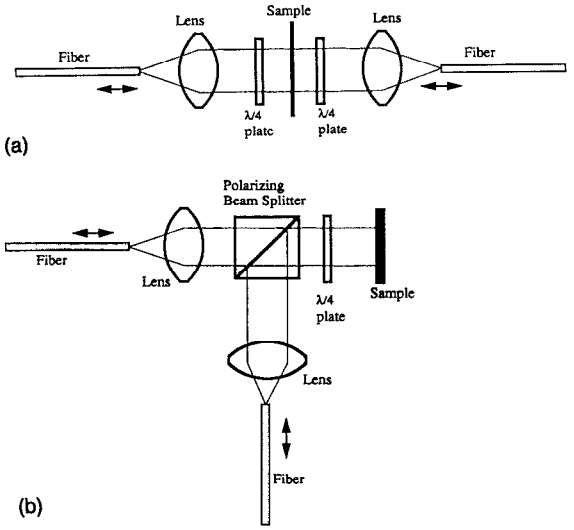

FIG. 2. Bulk optics inserted in the loop for (a) transmission and (b) reflection measurements.

lipticity, because magneto-optically induced ellipticity arises from nonreciprocal absorption, and consequently does not lead to a NRPS but to a small asymmetry in the absorption for the two polarization states.

We first describe the configuration which is used to measure the Faraday effect.[4] As explained above, we add in succession [see Fig. 2(a)] a quarter-wave (λ/4) plate, the sample holder, and another λ/4 plate, which comprise the bulk optics. Lenses are also added to focus the beams into the fiber. The polarization state in the fiber is linear, and the two λ/4 plates are arranged such that both beams are given circular polarization of the same handedness. We choose right-handed polarization states for the sake of discussion. With no sample, the clockwise propagating light is converted into right-handed circularly polarized light by the first λ/4 plate and converted back to the original linear state of polarization by the second λ/4 plate, and the counterclockwise propagating light will do the same, in the reverse direction. Assuming that no nonreciprocal phase shift occurs in the central portion of the bulk optics, then both clockwise and counterclockwise beams will emerge with no relative phase shift. If, however, a nonreciprocal phase shift occurs in the central portion of the bulk optics, one beam will be advanced in phase while the other will be retarded in phase, and the phase difference will be detected as an intensity change at the output of the interferometer.

To modify the apparatus for reflectance measurements, only one quarter-wave plate is needed, together with a polarizing cube beam splitter [Fig. 2(b)]. We set the linear polarization state in one fiber end to be parallel to the optical table, with the other orthogonal to it, and we use the beam splitter to selectively redirect one beam to overlap with the other. Each beam is given a different handedness upon passing through the λ/4 plate, which again is set to produce circular polarization states at the sample. If a perfect mirror is used as a sample, the handedness of each polarization state is switched upon reflection and the linear polarization which results from passing through the λ/4 plate a second time will

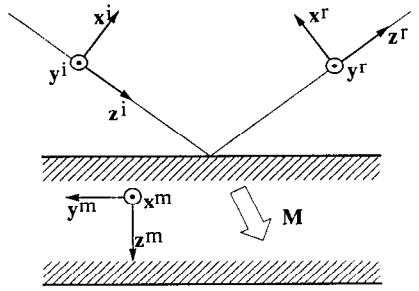

FIG. 3. Basic notations for components of incident and reflected beams from a magnetized surface.

be orthogonal to the original. Thus, the incident beam which is transmitted by the beam splitter is reflected by the beam splitter upon return, and vice versa, and a complete loop is established.

For the more general problem of measuring magneto-optic effects in the presence of linear birefringence, for arbitrary magnetization directions, and away from normal incidence, circular polarization states will no longer be eigenstates of the optical system, and we must search for the two polarization states which will lead to the largest signal. We describe the electric field of a plane wave as

$$\mathbf{E}(z,t)=\mathrm{Re}\{E_0\ \exp[i(\omega t-\phi)]\exp(-ikz)\}, \tag{2}$$

where $\mathbf{E}_0=E_x\hat{\mathbf{x}}+E_y\hat{\mathbf{y}}$ is the complex vector amplitude, and E_x and E_y are complex. We may then define the Cartesian Jones vector $\mathbf{E}$ as[10]

$$\mathbf{E}=\begin{bmatrix}E_x\\E_y\end{bmatrix}. \tag{3}$$

The action of optical elements on the polarization state may be described by complex 2×2 matrices acting on this vector, assuming that the wave retains its planar character. In Fig. 3 we define the coordinate systems which we shall use to describe the reflection of a plane wave from a magnetic surface. One of these, denoted by the superscript m, refers to the orientation of the magnetization vector in the medium, and the other two refer to the incident and reflected waves, $\mathbf{E}_1^i$ and $\mathbf{E}_1^r$.

The reflectivity matrix for a magnetized reflector, defined by the equation $\mathbf{E}^r=\mathbf{r}(\mathbf{M})\mathbf{E}^i$, is

$$\mathbf{r}(\mathbf{M})=\begin{pmatrix}\mathbf{r}_{pp}+a\mathbf{M}\cdot\mathbf{x}^m & b\mathbf{M}\cdot\mathbf{y}^m+c\mathbf{M}\cdot\mathbf{z}^m\\ -b\mathbf{M}\cdot\mathbf{y}^m+c\mathbf{M}\cdot\mathbf{z}^m & r_{ss}\end{pmatrix}, \tag{4}$$

where a, b, and c are complex coefficients which depend on the optical properties of the material and the experimental geometry, and are generally of order 10^{-3} or less, r_{ss} and r_{pp} are the diagonal elements of the reflectivity matrix for an unmagnetized material, and s and p refer to the usual s- and p-polarization convention. When the magnetization is oriented normal to the plane of incidence, which is the geometry of the transverse Kerr effect, we see that this matrix is diagonal and that the magnetization induces a small linear birefringence. This birefringence is linear in the magnetization, and is a truly nonreciprocal effect. For an appropriate choice of counterpropagating polarization states, the trans-

verse Kerr effect will lead to a nonreciprocal phase shift. Magnetization in the plane of incidence leads to nonzero off-diagonal terms, which are responsible for the well-known longitudinal and polar Kerr effects. In particular, the reflectivity matrix will be antisymmetric for magnetization oriented in the plane of the sample surface, and symmetric for magnetization oriented normal to the surface. Again, with the proper choice of polarization states, the nonreciprocal phase shift due to either one of these effects can be maximized. In fact, the symmetry properties of the reflectivity matrix are such that a measurement which is sensitive to the longitudinal effect is completely insensitive to the polar effect, and vice versa, whereas the transverse effect appears in both. By making measurements with three different sets of polarization states, we can completely determine the phase shift associated with each of these effects. In this way we may completely determine the magnetization vector, with no modification of the experimental geometry other than changing the orientations of the wave plates. Detailed analysis of the measurements required to make such a determination will appear in a subsequent publication.

III. NEAR-FIELD SAGNAC MAGNETO-OPTIC SENSOR

Resolution beyond the diffraction limit can be achieved with optical microscopy by operating in the near-field regime, where the evanescent components of the electromagnetic field strongly depend on the environment, i.e., the boundary conditions set by the sample with respect to the source.[11] In this near-field scanning optical microscopy mode (NSOM),[12] a subwavelength source and/or detector of visible light is placed in close proximity (of order of the size of d, the source) to a sample and raster scanned to generate images. The coupling of the near-field radiation to the far field is typically quite weak; the transmission coefficient at normal incidence has been calculated to be[11]

$$T=\frac{P_{\text{trans}}}{P_{\text{inc}}}\approx 10\left(\frac{d}{\lambda}\right)^6. \tag{5}$$

This is for the ideal case of a circular aperture in a perfectly conducting, infinitely thin screen, with diffraction-limited focusing of the radiation illuminating the pinhole; the problem is analogous to Rayleigh scattering (the additional factor of λ^{-2} comes from the illumination spot size). In general, the finite conductivity and thickness of the screen, as well as inefficiencies in the method used to deliver the incident light to the aperture, will lead to a reduction in this value. Recently, Betzig *et al.*[12] have demonstrated such a microscope with a spatial resolution of 120 Å, using as a light source a tapered optical fiber coated with aluminum. Polarization contrast has also been achieved by creating a polarized source and introducing a polarizer between the sample and the detector.[13] By orienting the polarizer near the extinction position, magneto-optic contrast with a resolution of 30–50 nm was observed in thin, transparent magnetic films.[14] Although some progress has been made in imaging opaque materials by using NSOM in reflection,[15–18] serious technical barriers impede similar studies of opaque magnetic samples, and to our knowledge none have been made.

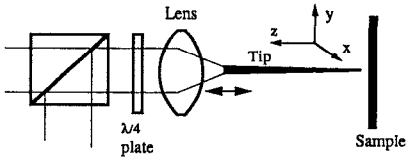

FIG. 4. Arrangement for near-field scanning in conjunction with reflection mode [Fig. 2(b)].

Many of the difficulties in achieving magneto-optic contrast NSOM in reflection are related to the crossed polarizer method for creating the contrast. Moreover, analysis of light scattered away from the normal of the sample is complicated by polarization state changes which are generally dominated by effects which have nothing to do with its magnetic state, such as the shape of the aperture, the direction of radiation in the far field, and the conductivities of both the sample and the tip. Light which reflects back through the aperture from which it came might carry fewer of these spurious polarization effects, but the problem of distinguishing the signal from an overwhelmingly large background becomes significant, since most of the light incident on the aperture is reflected without ever interacting with the sample. In other words, a large amount of "reciprocal" light is expected that will completely mask the real signal. We may expect the intensity which carries the signal to be a factor of 10^{-6} smaller than the incident intensity, and if we are to measure magneto-optic effects by analyzing this light with a crossed polarizer, we may expect a further reduction of 10^{-2}, so this is a formidable problem. One group[16,17] has succeeded in modulating the distance between the tip and the sample and using synchronous detection to attempt to solve this problem, but their resolution is not yet better than the diffraction limit and they have they have not yet addressed polarization effects.

The selective sensitivity of SMOS to nonreciprocal effects has led us to explore the possibility of using it as a detection scheme for NSOM with magneto-optic contrast in reflection. If we introduce an aperture between the focusing optics and the sample in Fig. 4 only the light generated in the near field of the magnetic sample will receive a nonreciprocal phase shift, and the enormous amount of background light which passes through reciprocal optics will go undetected. In fact, the presence of this more intense reciprocal radiation can actually serve to amplify the intensity change due to the small magneto-optic phase shift by means of an optical homodyne effect. Let us decompose the fields in the fiber loop into two components for each of the two counterpropagating waves,

$$E_1=A\ \exp(i\theta)+\alpha_+\ \exp(i\phi_+) \tag{6a}$$

and

$$E_2=A\ \exp(i\theta)+\alpha_-\ \exp(i\phi_-), \tag{6b}$$

where A and θ are the amplitude and phase of the reciprocal part of the fields, and $\alpha_\pm$ and $\phi_\pm$ are the amplitudes and phases of the nonreciprocal part. The nonreciprocal phase shift which we measure upon interfering these two waves will be

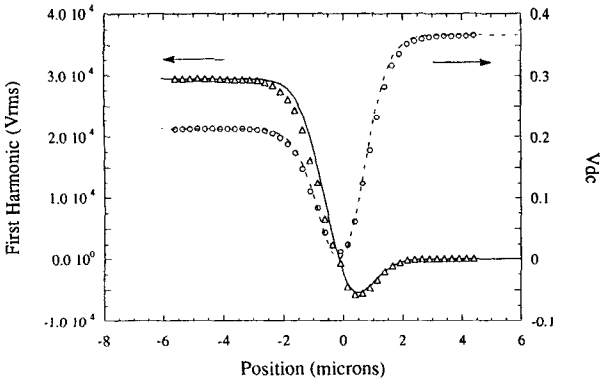

FIG. 5. First-harmonic and dc components of the detector voltage as the edge is traversed with the beam. The edge is at the center of the beam at a position of 0 and the beam is centered on the gold for positive values of the position. Solid and dashed lines represent the fit using Fourier optics analysis.

$$\Delta\phi = \arg\left(\frac{E_1}{E_2}\right) \cong \frac{2\alpha_{\text{avg}}}{A}\ \sin(\phi_+ - \phi_-)\cos(\phi_{\text{avg}} - \theta), \qquad (7)$$

where $\alpha_{\text{avg}} \equiv (\alpha_+ + \alpha_-)/2$, $\phi_{\text{avg}} \equiv (\phi_+ + \phi_-)/2$, and we have neglected higher-order terms. The signal which we measure is then

$$I_\omega \propto A^2 \Delta\phi = 2\alpha_{\text{avg}} A\ \sin(\phi_+ - \phi_-)\cos(\phi_{\text{avg}} - \theta), \qquad (8)$$

which is proportional to the field amplitude of the light reflected from the aperture, not the intensity. As a consequence, we may expect our signal to be orders of magnitude larger than NSOM in transmission, where the magneto-optic signal is proportional to the square of both the transmitted field amplitude and the magneto-optic phase shift, both small numbers. For a system which is limited by shot noise, this increase in signal will naturally be accompanied by a corresponding increase in noise, so that the signal-to-noise ratio will not change. However, the dramatic increase in signal strength allows us to move away from photomultiplier tubes to noisier but more convenient photodiode detection schemes.

To verify our analysis, we have deposited 2400 Å of TbFeCo on a silicon wafer, capped it with 200 Å of silicon nitride, then deposited 2000 Å of gold on top as a reflecting layer. We then etched 25 μm lines in the gold to expose the magneto-optic (MO) material, and scanned our beam across the edge dividing the gold from the MO material. The results of this scan are shown in Fig. 5, together with the response which we have calculated using standard Fourier optics techniques.[19] The first-harmonic signal, proportional to the NRPS, as well as the dc detector voltage, proportional to the average intensity, are plotted as a function of beam position on the sample, with the edge at zero. Note that as the edge approaches the center of the beam, both signals drop to zero. This is because the thickness of the gold plus the optical thickness of the nitride cap sum to almost exactly a quarter of one wavelength, so that there is a 180° phase shift between light reflected from the gold and light reflected from the MO material. When the edge is near the center of the beam, the reflected mode is almost fully antisymmetric about the plane of the edge and the optical axis, and the single-mode fiber rejects it. As the beam is moved onto the gold, the average intensity increases with the symmetric part of the reflected mode, and the first-harmonic signal crosses zero to become negative. This is exactly the optical homodyning effect described above: Although the bare MO signal is positive, when the wave reflected from the MO material is mixed with the stronger field reflected by the gold, the sign changes because the two waves are shifted relative to each other. In the theoretical fit, we have neglected aberrations in the focusing lens as well as the finite aperture of the lens. There is only one free parameter in the model, the beam radius, which takes a value of 2.2 μm in the curves shown; by simply calculating the magnification of our optics and assuming perfect lenses we obtain a radius of 1.7 μm. The agreement between theory and experiment is quite good, especially considering the limitations of a scalar theory in treating polarization properly.

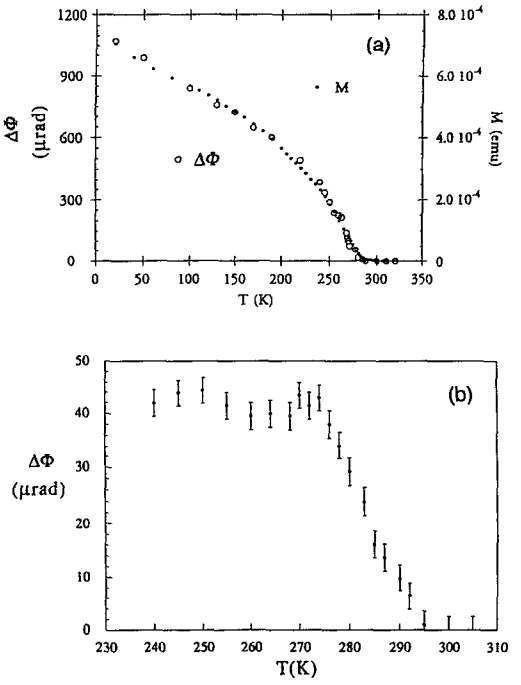

FIG. 6. (a) Transmission (Faraday) measurements and SQUID magnetometry on 480-Å-thick Gd film in an applied field of 30 Oe as a function of temperature. (b) Reflection phase shift using an applied field of 70 Oe.

IV. ADVANTAGES OF SMOS

As explained above, SMOS may achieve high sensitivity and high common-mode rejection for reciprocal effects. The ultimate limit on our sensitivity will be set by the shot noise of the laser. For optical powers of ~1 mW at the detector, the shot-noise-limited sensitivity is ~50 nrad/$\sqrt{\text{Hz}}$. In Fig. 6(a) we show Faraday and superconducting quantum interference device (SQUID) magnetization measurements from 400 Å Gd film. The magnetization lies in the plane, and the Faraday effect measurements have been made in zero field with the sample oriented at 45° to the optical beam. However, the most striking example of the current sensitivity of the appa-

ratus is shown in Fig. 6(b), where the Kerr effect of this 400 Å Gd film is measured through the ferromagnetic transition (T_c=270 K) with only a 70 Oe applied field, with a measurement time of 10 s per point. Currently, we have achieved a NRPS sensitivity of 2 μrad/$\sqrt{\text{Hz}}$ in transmission and 4 μrad/$\sqrt{\text{Hz}}$ in reflection. The sensitivity may be increased toward the shot-noise limit with some improvements in the construction of the apparatus and in particular the power and spectral characteristics of the source.

An important feature of the Sagnac loop is its immunity to reciprocal effects such as linear birefringence or optical activity. This immunity comes from the fact that two beams are experiencing the same optical path, and phase shifts that do not come from broken time-reversal symmetry will exactly cancel each other. This immunity may be particularly important for evaluation of anisotropic materials where birefringence may be difficult to differentiate from Kerr or Faraday effects if not analyzed properly.

Based on the advantages of the SMOS, it is clear that many of the difficulties with doing magneto-optic contrast NSOM in reflection may be eliminated. If SMOS is used, the background light, as much distorted as it may be, will not lead to a background signal. On the contrary, this light serves to amplify the magneto-optically induced signal by orders of magnitude. Moreover, the high sensitivity allows for relatively easier detection of the very small signals. We believe that this method provides an excellent scheme for expanding the potential applications of NSOM.

The advantages of the near-field SMOS (NFSMOS) microscope over other spin-polarized devices are evident. First is the possible high sensitivity, in particular for materials with large magneto-optic coefficient. The second is the spatial resolution. Current near-field optical microscopes reach a spatial resolution of 120 Å. This is smaller than a typical superparamagnetic size and thus extremely useful for the detection of magnetism. Moreover, since the detection is made with light, the relevant probing thickness is of order of optical penetration depth, hence information from deeper than the first few atomic layers can be obtained. Finally, the accumulation of data can be obtained much faster with improvements in efficiency. Thus, one may envision using this method for high-frequency measurements.

V. SUMMARY

The above instrument opens for us new avenues in the research of magnetic materials. In particular we believe that because of the complete rejection of any reciprocal optical effects, the instrument is ideal for use in reflection mode in a near-field configuration. In this way, it may be possible to do magneto-optics on a scale of ~200 Å (*current near-field microscopy using tips that preserve polarization may go to a length scale of ~120 Å*). This could potentially lead to new opportunities in high-density magnetic recording and magneto-optic readout.

ACKNOWLEDGMENTS

We would like to thank Michael Farle for equipment and useful discussion, as well as Federico Sequeda for fabricating the TbFeCo wafer. We would also like to acknowledge the fruitful collaborations along many phases of this work, in particular with S. Spielman and T. Geballe. Parts of this work were supported by AFOSR, by NSF through the Center for Materials Research at Stanford University, by a special grant from IBM, and by a grant from Stanford Office for Technology Licencing.

[1] L. M. Falicov, D. T. Pierce, S. D. Bader, R. Gronsky, K. B. Hathaway, H. J. Hopster, D. N. Lambeth, S. S. P. Parkin, G. Prinz, M. Salamon, I. K. Schuller, and R. H. Victora, J. Mater. Res. **5**, 1299 (1990); S. D. Bader, Proc. **78**, 909 (1990).
[2] See, for example, C. A. Ballentine, R. L. Fink, J. Araya-Pochet, and J. L. Erskine, Appl. Phys. A **49**, 459 (1989); S. D. Bader and E. R. Moog, J. Appl. Phys. **61**, 3729 (1987).
[3] See, for example, M. J. Freiser, IEEE Trans. Magn. **MAG-4**, 152 (1968).
[4] S. Spielman, K. Fesler, C. B. Eom, T. H. Geballe, M. M. Fejer, and A. Kapitulnik, Phys. Rev. Lett. **65**, 123 (1990).
[5] S. Spielman, J. S. Dodge, K. Fesler, L. W. Lombardo, M. M. Fejer, T. H. Geballe, and A. Kapitulnik, Phys. Rev. B **45**, 3149 (1992).
[6] S. Spielman, J. S. Dodge, L. W. Lombardo, C. B. Eom, M. M. Fejer, T. H. Geballe, and A. Kapitulnik, Phys. Rev. Lett. **68**, 3472 (1992).
[7] S. Doniach, A. Kapitulnik, P. Frank, M. M. Fejer, S. Spielman and S. Dodge, in *Physical Phenomena at High Magnetic Fields*, edited by E. Manousakis, P. Schlottmann, P. Kumar, K. S. Bedell, and F. M. Mueller (Addison-Wesley, Reading, MA, 1992).
[8] See, for example, papers in *Fiber-Optic Rotation Sensors and Related Technologies*, edited by S. Ezekiel and H. J. Arditty (Springer, Berlin, 1982).
[9] L. D. Landau, E. M. Lifshitz, and L. P. Pitaevskii, *Electrodynamics of Continuous Media*, 2nd ed. (Pergamon, Oxford, 1984), p. 347.
[10] R. M. A. Azzam and N. M. Bashara, *Ellipsometry and Polarized Light* (North-Holland, Amsterdam, 1989).
[11] H. A. Bethe, Phys. Rev. **66**, 163 (1944).
[12] E. Betzig, J. K. Trautman, T. D. Harris, and J. S. Weiner, and R. L. Kostelak, Science **251**, 1468 (1991).
[13] E. Betzig, J. K. Trauman, J. S. Weiner, T. D. Harris, and R. Wolfe, Appl. Opt. **31**, 4563 (1992).
[14] E. Betzig, J. K. Trautman, R. Wolfe, E. M. Gyorgy, P. L. Finn, M. H. Kryder, and C.-H. Chang, Appl. Phys. Lett. **61**, 142 (1992).
[15] J. K. Trautman, E. Betzig, J. S. Weiner, D. J. DiGiovanni, T. D. Harris, F. Hellman, and E. M. Gyorgy, J. Appl. Phys. **71**, 4659 (1992).
[16] D. Courjon, J.-M. Vigoureux, M. Spajer, K. Sarayeddine, and S. Leblanc, Appl. Opt. **29**, 3734 (1990).
[17] M. Spajer, D. Courjon, K. Sarayeddine, A. Jalocha, and J.-M. Vigoureux, J. Phys. (Paris) III **1**, 1 (1991).
[18] U. C. Fischer, J. Vac. Sci. Technol. B **3**, 386 (1985).
[19] S. Spielman, Ph.D. thesis, Stanford University, 1992.